Justification for the use of Markovian Langevin statistics in the modelling of activated surface diffusion.

J. Wilkinson[1] J. Ellis[1]

[1] Cavendish Laboratory, JJ Thomson Avenue, Cambridge CB3 0HE, UK

December 15, 2021

Abstract (195 words)

Low temperature surface diffusion is driven by the thermally activated hopping of adatoms between adsorption sites. Helium spin-echo techniques, capable of measuring the sub-picosecond motion of individual adatoms, have enabled the bench-marking of many important adsorbate-substrate properties. The well-known Markovian Langevin equation has emerged as the standard tool for the interpretation of such experimental data, replacing adatom-substrate interactions with stochastic white noise and linear friction. However, the consequences of ignoring the colored noise spectrum and non-linearities inherent to surface systems are not known. Through the computational study of three alternative models of adatom motion, we show that the hopping rate and jump distributions of an adatom are fixed to within a few percent by the potential energy surface and a new generalized energy exchange rate parameter alone, independent of the model used. This result justifies the use of the Markovian Langevin equation, regardless of the true statistical nature of adatom forces, provided results are quoted in terms of the new energy exchange rate parameter. Moreover, numerous mechanisms for the effect of noise correlations and non-linear friction on the energy exchange rate are proposed which likely contribute to activated surface diffusion and activated processes more generally.

Introduction (571 words)

Diffusion on the atomic scale is distinguished from the diffusion of larger particles as the potential generated by the medium cannot be considered homogeneous at this scale.[1] The regular periodic potential formed by a crystalline substrate results in a form of activated diffusion where adatoms become bound to and hop between local adsorption sites. The motion observed through helium scattering is therefore far more sophisticated than the archetypal diffusion of the Einstein-Smoluchowski type through a homogeneous fluid.[2]

The information contained in helium spin-echo measurements is sufficient to benchmark many important properties of the adatom-substrate interaction. These include the activation barrier to diffusion, adatom vibrational frequencies, the rate of hopping between sites, and the strength of atomic scale friction.[3–6] These properties are consequential for the development of many technologies and the results of helium spin-echo experiments have contributed to the understanding of graphene growth, self-assembling organic semiconductors, and the design of topological insulators.[7–10] A thorough understanding of how to model activated diffusion processes and interpret the important quantities involved is therefore of wide interest.

The standard approach to modelling diffusive motion uses a Markovian Langevin equation to reduce the forces of a large complex heat bath on a particle of interest to a simple Markovian stochastic force and a dissipative linear friction.[11–13] This approach is used in the interpretation of almost all helium spin-echo data[2,3] despite numerous properties of adatom diffusion being in direct conflict with the assumptions used to construct the Markovian Langevin equation. For instance, the white noise power spectrum implied by the Markovian approximation cannot exist on a real substrate since the dominant source of noise, surface phonons,[14] cannot vibrate faster than the Debye phonon cutoff frequency. The cutoff frequency of most lighter metals is around $6-10\text{THz}$,[15–18] which is not significantly faster than typical adatom vibrational frequencies of $1-4\text{THz}$.[19–21] The Debye frequency of heavier metals such as lead and rubidium is found to dip into the low terahertz range,[22,23] making the approximation that adatom motion is effectively driven by white noise manifestly false. The fact that all real forms of noise are band-limited is a negligible detail for most forms of unactivated long-time diffusion.[24,25] However, even without the complications of atomic scale interactions, some phenomena, such as anomalous sub-diffusion through viscoelastic fluids, can only be accounted for through the use of a generalized non-Markovian Langevin equation.[13,25,26] The assumption of a linear friction force is also difficult to justify since the exact trajectories of adatoms are not experimentally accessible. From a theoretical perspective, there is no a priori reason for the vanishing of higher powers of velocity in the friction force.[11] The laws of equilibrium thermodynamics can be satisfied by a large number of non-linear friction laws with linear friction being nothing more than the simplest possible case.

If the forces on an adatom do not resemble Markovian Langevin statistics, the question arises, to what extent are the wide array of results derived from the Langevin equation in activated dynamics meaningful at all? We address

this concern through the computational study of alternative models of diffusion which explore the effect of noise correlations and non-linear force laws on activated diffusion. We demonstrate that the details of adatom motion can have a significant effect on hopping behavior, however, only through changing the effective energy exchange rate with the substrate. The results derived through Markovian Langevin simulations are therefore valid provided they are quoted in terms of the new generalized energy exchange rate parameter.

Definitions & computational models (704 words)

With the notable exception of Hydrogen adsorbates,[27] surface diffusion is predominantly a classical activated diffusion process. The hopping rate and distribution of jump lengths fully specify the rate of macroscopic diffusion over the surface. Both are strongly influenced by the shape of the trapping well, in particular the activation energy, as well as the rate at which the adatom exchanges energy with the substrate. The rate of hopping, γ, is usually observed to obey an Arrhenius law, of the form $\gamma = \gamma_0 \exp\left(-E_a/k_BT\right)$, with an associated activation energy, E_a and a pre-exponential factor γ_0. While it is relatively simple to extract an activation energy directly from experimental data,[28,29] it is not possible to disentangle the energy exchange rate of the system from other effects which contribute to the pre-exponential factor without making further assumptions. The most common approach assumes that the force on an adatom of mass m may be treated as a random variable obeying the Markovian Langevin equation in a background potential $U(\vec{r})$,

$$\begin{aligned} m\ddot{\vec{r}} &= -m\eta\dot{\vec{r}} - \nabla U(\vec{r}) + \vec{f}(t) \\ \text{where } \langle f(t_1)f(t_2)\rangle &= 2k_BTm\eta\delta(t_1-t_2), \end{aligned} \tag{1}$$

and to fit the experimental data with simulated solutions to the Langevin equation. The resulting best fit friction parameter, η, parameterizes the strength of the random force $\vec{f}$ and may be used as a quantifier of the rate of energy transfer with the substrate. This approach is used in the analysis of almost all helium spin-echo data.[2,3]

In addition to the Markovian Langevin equation, we present three models for the motion of adatoms. The first relaxes the Markovian approximation by introducing a correlated noise force with an autocorrelation function given by a memory kernel, $K(t)$. The second fluctuation-dissipation theorem requires that both the friction force and the noise force be modified, resulting in the generalized Langevin equation,[13]

$$\begin{aligned} m\ddot{\vec{r}} &= -m\eta\int_{-\infty}^{t} \mathrm{d}t' K(t-t')\dot{\vec{r}}(t') - \nabla U(\vec{r}) + \vec{f}(t) \\ \text{where } \langle f_i(t_1)f_j(t_2)\rangle &= 2k_BTm\eta K(|t_1-t_2|)\delta_{ij}. \end{aligned} \tag{2}$$

A causal exponential memory kernel, $K(t>0) = \frac{1}{\tau}\exp\left(-\frac{t}{\tau}\right)$ and $K(t<0) = 0$, parameterized by a noise correlation time τ was used to generate a Lorentzian noise power spectrum,

$$\left\langle |\tilde{f}_i(\omega)|^2 \right\rangle \propto \frac{1}{1+\omega^2\tau^2}. \tag{3}$$

In the limiting case of $\tau = 0$, the white noise of the Markovian Langevin equation is recovered.

The second model explores the effects of non-linear friction through a cubic friction law parameterized by ζ,[11]

$$\begin{aligned} m\ddot{\vec{r}} &= -m\zeta\dot{r}^2\dot{\vec{r}} - \nabla U(\vec{r}) + \vec{f}(t) \text{ where} \\ \langle f_i(t_1)f_j(t_2)\rangle &= \left(4\zeta\left(k_BT\right)^2 + 2m\zeta\left(k_BT\right)\dot{r}^2(t_1)\right)\delta\left(t_1-t_2\right)\delta_{ij}. \end{aligned} \tag{4}$$

In general, such a friction law may also contain a linear component, however, we primarily present the results of pure cubic friction as an extreme case with no resemblance to the commonly used linear friction. The full linear-cubic friction equation and its associated fluctuation-dissipation relation may be found in work by Kramers.[11]

The final model presented is a full 3D molecular dynamics simulation of sodium on copper(001) which tracks the harmonic interactions and motion of each copper atom in an $8\times8\times8$ substrate as well as the interactions with a sodium adatom via a Morse potential. The simulation parameters determined by Ellis and Toennies were optimized to fit the binding energy, activation energy, and vibrational frequencies of Na on Cu(001).[30] This model reproduces the phonon dispersion relation of a real copper crystal[15] and therefore provides a realistic model of three dimensional phonon-adatom interactions. Interactions with the surface electron cloud, which have a secondary effect in sodium on copper(001),[14] are not accounted for.

The two dimensional free energy surface parallel to the substrate was extracted from the 3D simulation through the density function of a canonical ensemble of trajectories and the definition (discussed in further detail the methods section),

$$U_{\text{free}}(\vec{x}) = -k_BT\log\left(\left\langle\delta^{(2)}(\vec{r}_{\parallel}(t)-\vec{x})\right\rangle\right). \tag{5}$$

The extracted potential, shown in Fig. 1, was used as the background potential of the Langevin type simulations and ensures that each model attains the same two dimensional Boltzmannian equilibrium phase space distribution, albeit through fundamentally distinct microscopic statistics. The mass of the adatom in each simulation was set to the mass of sodium, 23u.

The absence of a linear Markovian friction in these alternative models necessitates the introduction of a generalized energy exchange rate parameter. We define the energy exchange rate as the inverse of the correlation time, ϕ, of the *total energy* autocorrelation function,

$$\frac{\langle E(t)E(0)\rangle - \langle E\rangle^2}{\langle E^2\rangle - \langle E\rangle^2}, \tag{6}$$

as defined in Fig. 2. The energy exchange rate defined through ϕ^{-1} has the advantage of being applicable to any model of diffusion while coinciding with η in the case of a

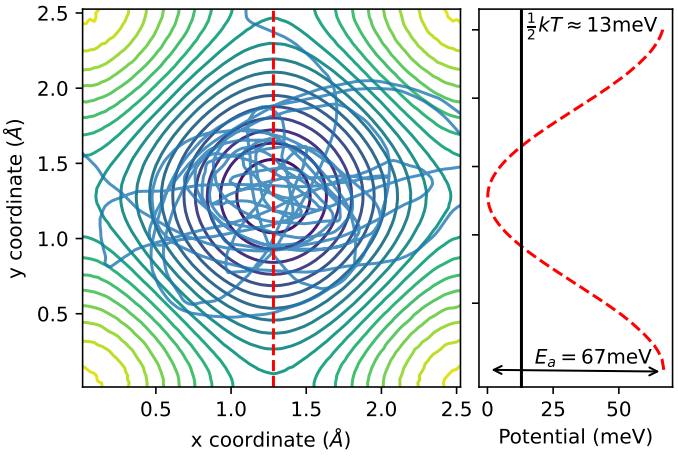

Figure 1: **Visualization of adatom motion over a potential surface.** The potential energy surface, U_{free}, extracted from the sodium on copper(001) 3D molecular dynamics simulation is shown alongside a superimposed trajectory typical for a low friction activated diffusion process. The red dashed line in the right panel shows a cross-section of the potential through an adsorption site and two bridge sites as annotated in the panel on the left.

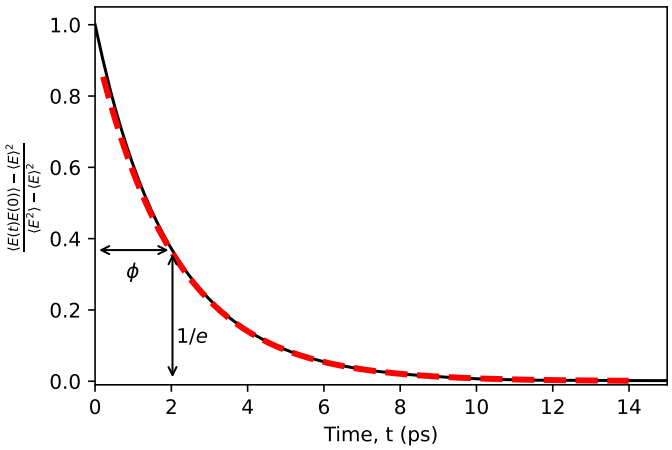

Figure 2: **Definition of the generalized energy exchange rate, ϕ^{-1}.** A typical normalized total energy autocorrelation function is shown. Since the total energy autocorrelation function is generally not a pure exponential, as shown by the fit in red, the energy exchange rate, ϕ^{-1}, is defined as the reciprocal of the time taken for the function to fall by a factor of $\frac{1}{e}$.

Markovian Langevin equation in a harmonic well. The total energy autocorrelation function of the 3D simulation contains an additional very rapid decorrelation at short times attributed to interactions with the third coordinate. To compensate for this effect, the decorrelation time of the long-time exponential tail was used in the case of the 3D simulation (further discussion in the supplemental information).

Hopping rates (789 words)

Each simulation was run repeatedly at 300K for a total run time of up to 2µs per configuration. The hopping behavior of each simulated adatom was evaluated using the observable quantity in a surface scattering experiment, the intermediate scattering function,

$$\text{ISF}(\Delta\vec{K}, t) = \left\langle \exp\left(i\Delta\vec{K}\cdot\vec{r}(t)\right)\right\rangle. \qquad (7)$$

A typical ISF for a fixed momentum transfer, $\Delta\vec{K}$, is shown in the main axes of Fig. 3. In the case of activated diffusion, the long time decay rate of the ISF, Γ, is proportional to the adatom hopping rate, and the shape of Γ as a function of ΔK, as shown in the inset of Fig. 3, is set by the distribution of jump lengths.[28,31]

As a measure of the total hopping rate, the peak of the jump distribution, Γ_{max} (annotated in Fig. 3), was calculated for each model and summarized in Fig. 4 as a function of the new energy exchange rate parameter. The results cover almost an order of magnitude of hopping rates as a function of the various model parameters. Despite the wide range of simulated hopping rates, the striking feature of Fig. 4 is that at a fixed energy exchange rate, all

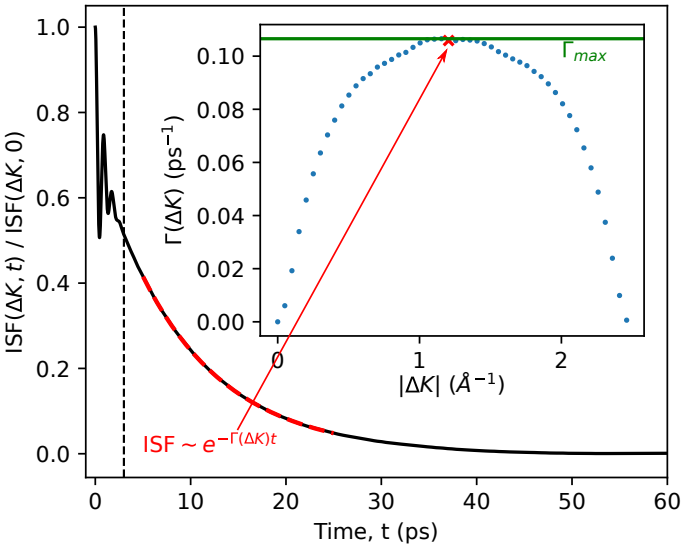

Figure 3: **Definition of basic surface scattering observables.** The main axes show a typical ISF over time for a fixed momentum transfer. The decay rate, Γ, of the ISF's exponential tail is proportional to the hopping rate of the adatom. The inset axes show a jump distribution obtained by calculating Γ over a range of momentum transfers. The shape of the jump distribution is set by the distribution of adatom jump lengths. All ISFs presented in this paper are quoted with the a momentum transfer pointing from the adsorption site through one of the equivalent bridge sites.

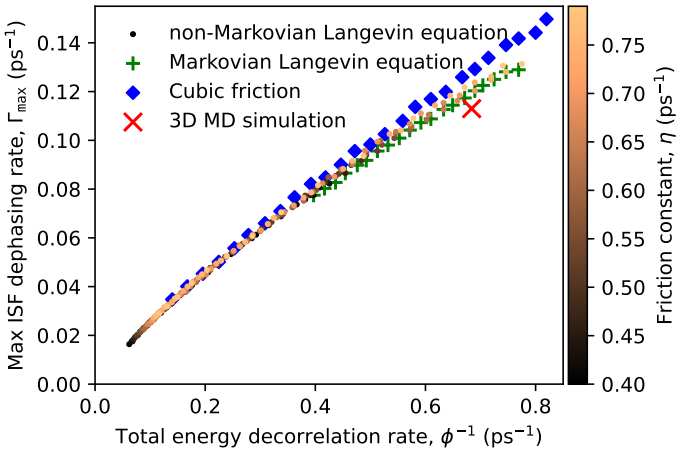

Figure 4: **A comparison of each model's overall hopping rate dependence on the generalized energy exchange rate, ϕ^{-1}.** For each model, the maximum ISF dephasing rate, $\Gamma_{\max}$, is plotted against the energy exchange rate, ϕ^{-1}. The grouping of the models at fixed ϕ^{-1} demonstrates that the ISF dephasing rate is predominantly set by the energy exchange rate and the 2D potential background. Other microscopic details account for less than 3% of the variance in the limit of low energy exchange rate. The value of η used in the non-Markovian simulation is insufficient to specify the hopping rate, as indicated by the point color.

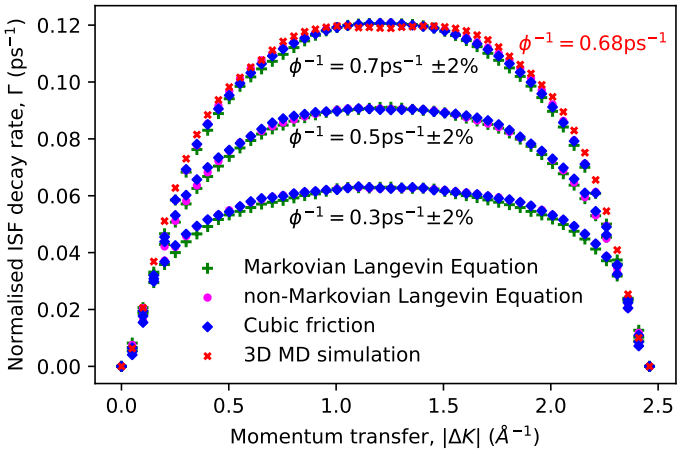

Figure 5: **A comparison of each model's jump distribution at a fixed generalized energy exchange rate, ϕ^{-1}.** Each set of points show the jump distribution of a particular model for three energy exchange rates: $\phi^{-1} = 0.3$, 0.5 and 0.7ps^{-1}. A noise correlation time of $\tau = 0.1$ps was used for the non-Markovian model in each instance. The jump distributions show very little variation across the models at a fixed energy exchange rate.

adatoms appear to hop at approximately the same rate, regardless of the friction law or noise correlation time used. For instance, the color of non-Markovian model's markers show that, for fixed η, the total hopping rate can vary by many multiples when the noise correlation time is adjusted. However, when considered as a function of a fixed energy exchange rate, the hopping rate is found to vary by less than 3%, regardless of τ. Noise correlations therefore do in fact have an effect on an adatom's hopping rate, but to first order, this effect only occurs through the energy exchange rate and may be compensated for through a corresponding adjustment of η. Remarkably, there does not appear to be a large behavioral difference between the linear and cubic friction models either. Despite using a fundamentally distinct law of friction, the cubic model's hopping rate was found to follow a very similar trend to that of the linear models as a function of ϕ^{-1}. The agreement is particularly good in the low energy exchange rate limit where there is no discernible effect of using cubic over linear friction. Even the 3D model, which likely has a unique law of dissipation and contains sophisticated noise correlations was found to hop at a rate within 6% of a Markovian Langevin simulation with an analogous energy exchange rate. We conclude that as far as the hopping rate is concerned, the parameter which matters most is the energy exchange rate and the details of how the energy is transferred are mostly inconsequential.

The shape of the jump distribution of each model was compared by tuning the available parameters to run each model over a fixed set of energy exchange rates. The jump distributions for each model at the energy exchange rate of approximately 0.3, 0.5, and 0.7ps^{-1} are shown in Fig. 5. Since the variation of amplitudes is quantified in Fig. 4, the jump distributions presented are normalized to peak at the same height within each energy transfer rate to allow for the comparison of the jump distribution shape. For a fixed energy exchange rate, the adatom jump distributions were found to agree well across all models with only small differences in shape. The peaks of the jump distributions at higher exchange rates are all observed to be narrower than those at lower exchange rates, indicating a decrease in the probability of multiple hops.[28] The narrowing effect is expected since higher energy exchange rates decrease the probability that a high energy particle which has escaped its adsorption site finds another transition site before thermalizing. The largest deviation is seen in the 3D model with a greater proportion of adatom jumps terminating outside of the adjacent adsorption sites compared to the 2D models, although the difference is not large.

These results provide strong evidence that the hopping rate and jump distribution of a low-friction activated diffusion model are fixed by the 2D potential energy surface and the energy exchange rate alone, with almost complete independence of any other details in the low exchange rate limit. The slightly larger deviations of the 3D model are not well understood but are likely due to additional memory effects as a result of energy exchange with the third co-ordinate and the 3D details of the potential affecting

the probability of escape when enough energy is obtained. Furthermore the deviations seen across the board are well within the accuracy of current experimental techniques and therefore would not be observable within an experimental context. Evidently, all the results derived from the Markovian Langevin equation so far remain completely valid, not because the underlying system is necessarily described by the Markovian Langevin equation, but rather that the energy exchange rate obtained is correct, regardless of the underlying statistics.

Energy exchange rates (1069 words)

Having established the generalized energy exchange rate as a quantity of interest, we shift focus to evaluating the effects which contribute to ϕ^{-1}. The introduction of noise correlations was found to suppresses the energy exchange rate with the substrate, as shown in Fig. 6a. For the sake of comparison, the red line shows the energy exchange rate of a particle with Markovian Langevin statistics in a harmonic well, $\phi^{-1} = \eta$. For short correlation times, we find the energy exchange rate is close to η, but even for $\tau = 0$, there are small differences due to anharmonicities in the background potential. As the noise correlation time approaches 0.4ps, the energy exchange rate is seen to fall by close to a factor of four, demonstrating that the narrowing of the noise power spectrum can have a large effect on the energy exchange rate. Regardless of the noise correlation time, the exchange rate was found to remain linear in η suggesting that η continues to act as an overall interaction strength parameter while τ controls the cutoff frequency of available noise modes.

The linear dependence of ϕ^{-1} on η inspires the introduction of a dimensionless, η independent, suppression factor $I = \frac{\phi^{-1}}{\eta}$ which quantifies the suppression of energy exchange as a function of τ. The suppression factor for the non-Markovian simulation is shown in Fig. 6b alongside the analytically derived suppression factor of an equivalent non-Markovian particle in a harmonic well evaluated at two natural frequencies, ω_0 and ω_1. The toy model, solved in the supplemental information, is found to admit a similar η independent suppression factor in the low friction limit. When the the toy model is evaluated with the natural frequency, ω_0, implied by the curvature of the minimum of U_{free}, there is strong qualitative agreement, however the model appears to underestimate the suppression factor. Interestingly, when evaluated with a natural frequency, ω_1, reduced by 30%, there is far better quantitative agreement, likely compensating for some an-harmonicities in background potential. The qualitative agreement of the suppression factors nevertheless indicates a similar underlying origin. The suppression effect can be understood by considering the expected energy change of the adatom when subjected to a single noise impulse which decays in time as $K(t)$. Without loss of generality, we suppose the impulse is imparted in the direction of the instantaneous velocity. If $K(t)$ decays quickly compared to the oscillation period, then the impulse is imparted entirely in the direction of motion, and the adatom quickly settles into a new, higher energy level. If $K(t)$ decays at a rate comparable to the oscillation period of the well then some of the energy imparted initially is removed when the force acts against the direction of motion as the adatom swings back. The new energy level attained is therefore not as high as in the former case and we expect a lower change in the total energy per impulse. A similar argument can be made for the correlated friction force removing less energy per oscillation. This interpretation is reflected in the mathematical form of the low friction approximation of the harmonic well's suppression factor as an oscillating integral over $K(t)$,

$$I(\tau, \omega_0) = \int_0^\infty \mathrm{d}t K(t) \cos\omega_0 t = \mathrm{Re}\left(\tilde{K}(\omega_0)\right) = \frac{1}{1 + (\omega_0 \tau)^2}. \tag{8}$$

For an exponential memory kernel, the suppression factor coincides exactly with the power spectrum of the memory kernel, however in general this is not the case. In the supplemental information we show more generally that, in the low-friction limit, the suppression factor in a harmonic well with an arbitrary memory kernel is given by the form of the power spectrum of the noise around ω_0,

$$I(\omega_0) = \mathcal{F}\{K(|t|)\}(\omega_0) = \frac{\left\langle |\tilde{f}(\omega_0)|^2 \right\rangle}{4\pi k_B T m \eta}. \tag{9}$$

Moreover, the noise power spectrum in a physical system is likely to exhibit a much sharper cutoff than the Lorentzian spectrum of an exponential memory kernel. Fig. 6c contrasts the power spectrum of the force experienced by an adatom held stationary at an equilibrium point of the 3D simulation compared to the Lorentzian spectrum used in our non-Markovian simulations. This spectrum is feature rich but clearly demonstrates a sharp cutoff around the copper cutoff frequency of 7.4THz. The corresponding time domain noise autocorrelation function contains clear oscillations on the order of a few terahertz. By tuning the mass of the adatom in the 3D simulation, a doubling in the energy exchange rate has been observed when the frequency of the noise correlation oscillations match the adatom's vibrational frequencies, compared to $m = 23$u. This effect warrants its own investigation but is included here to demonstrate that the effect of noise correlations is likely meaningful in the context of realistic phonon-adatom interactions. High atomic mass substrates with low phonon cutoff frequencies such as lead or rubidium paired with light adatoms may result in the conditions needed to measure systematic changes to the hopping pre-exponential factor when the timescale of adatom vibrational frequencies match features in the the noise spectrum. It is unknown whether the effect would be visible over the other differences in such systems.

Since any realistic non-linear model of friction is likely to contain both linear and non-linear contributions, the energy exchange rate of the cubic model in Fig. 6d is shown alongside a set of simulations run with a combination of linear and cubic friction. The strength of the linear term was set to $\eta = 0.4\text{ps}^{-1}$ which coincides with the y-intercept of the linear fit to the blue points in Fig. 6d. Furthermore,

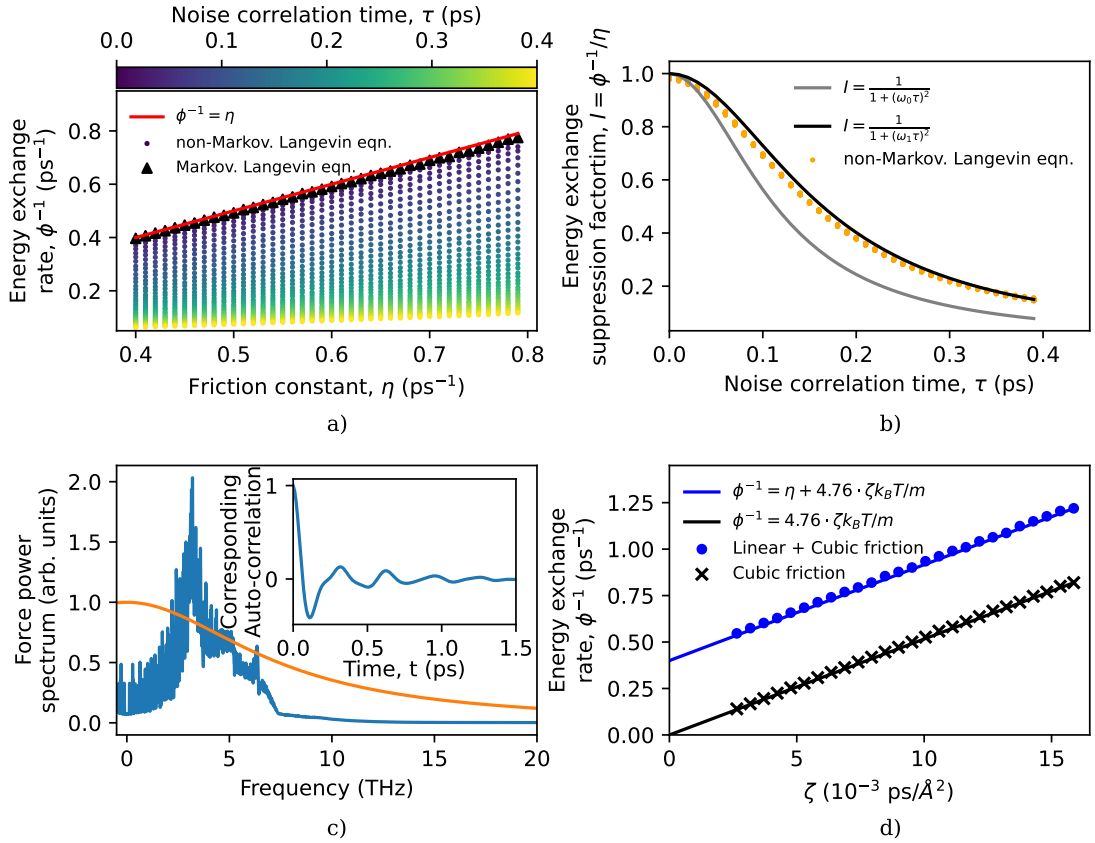

Figure 6: **Factors influencing the generalized energy exchange rate.** **a**, the energy exchange rate as a function of the friction parameter and noise correlation time in the linear friction Langevin models. **b**, the suppression factor, $I = \phi^{-1}/\eta$, of the non-Markovian Langevin model is shown in orange points. The grey line shows shows the suppression factor in a toy model of an equivalent non-Markovian Langevin equation in a harmonic potential of equilibrium natural frequency, $\omega_0 = 8.8\text{ps}^{-1}$, matching the curvature of U_{free}. The black line shows the suppression factor of the same toy model with a reduced natural frequency of $\omega_1 = 6.1\text{ps}^{-1}$. **c**, In orange, the form of a Lorentzian power spectrum used in the non-Markovian simulations alongside the power spectrum of the force seen by an adatom held fixed at the minimum of an adsorption site in the 3D simulation. Inset in **c** is the corresponding time-domain noise autocorrelation function for the force at the equilibrium point of the 3D model. **d**, in black markers, the energy exchange rate of the cubic friction model as a function of the cubic friction coupling constant. In blue markers, the energy exchange rate of a Langevin simulation run with a combination of cubic and linear friction with $\eta = 0.4\text{ps}^{-1}$. Each solid line shows an expression for the energy exchange rate as as a function of η and ζ obtained through dimensional analysis and a linear fit to determine the proportionality constant $A = 4.76$.

the gradient of ϕ^{-1} as a function of ζ is found to be independent of η. The implied affine relationship suggests ϕ^{-1} may be separated out in a lowest order expansion in the friction constants. Although cubic friction is much more difficult to analyze analytically, simple dimensional analysis on the co-efficient of ζ in the expansion of ϕ^{-1} requires,

$$\phi^{-1} = \eta + A\frac{k_B T}{m}\zeta + \ldots, \tag{10}$$

where A is a dimensionless functional of the potential U_{free}. Fig. 6d implies $A = 4.76$ for the given system. With the exception of background potential anharmonicities, none of the analysis presented up to this point has suggested any temperature dependence of the energy exchange rate. However, in the case of Eq. 10, the temperature is required to account for the dimensions of ζ. Previous work on the Markovian Langevin equation in surface dynamics by Diamant et al. highlighted an anomalous temperature dependence of the linear friction required to fit the same 3D simulation of sodium on copper(001) presented here.[28] We propose that the effect observed by Diamant et al. was in fact a temperature dependent energy exchange rate as a result of cubic contributions to the friction in the 3D model. The data provided by Diamant et al. together with Eq. 10 enables an estimate of the magnitude of cubic forces in the 3D model at thermal velocities,

$$\left\langle \frac{m\zeta|\dot{\vec{r}}|^3}{m\eta|\dot{\vec{r}}|} \right\rangle = \frac{2k_B T\zeta}{m\eta} \approx 0.23, \tag{11}$$

where $\frac{1}{2}m\left\langle|\dot{\vec{r}}|^2\right\rangle = kT$ in two dimensions. Our estimates indicate the observed temperature dependence may be achieved using $\zeta = 6.4 \times 10^{-3}\text{ps}\,\text{Å}^{-2}$ and $\eta = 0.37\text{ps}^{-1}$.

Discussion (350 words)

The results presented re-affirm that the single energy exchange rate parameter obtained through the Markovian Langevin equation is sufficient for describing the transport properties of low friction activated surface diffusion. However, the energy exchange rate must be interpreted as an aggregation of subtle microscopic details, the breakdown of which may not be knowable and may vary as a function of temperature. Although the ability to extract useful information from a system with sophisticated microscopic statistics using a simple Markovian Langevin equation is an interesting result in its own right, the goal of scientific modelling is to construct models which can make causal predictions. This aim warrants a discussion of the features of surface reactions which might be missed in simulations using the Markovian Langevin equation. The most important determinants of the rate of chemical reactions on a surface are the distribution of reagents in position space, how much energy they have, and the rate of replenishment of spent reagents through macroscopic transport over the surface. The results presented demonstrate that a Markovian Langevin equation equipped with the correct energy exchange rate gets precisely this right. For simple monatomic species at low coverage, this is likely the end of the story and the Markovian Langevin equation can likely be safely used for the prediction of surface processes. We however make the final comment that the reactions of larger molecules is influenced by their conformational mobility. Kramers' theory of reaction rates treats the contortion of molecules as a diffusive process in its own right, driven by Markovian noise.[11,12] Within Kramers' model, the energy exchange effects we have demonstrated therefore play a role and inspire various possible generalizations of Kramers' low friction escape rate formula. While the timescale of most molecular vibrations is much greater than the phonon cutoff frequency of a substrate, there are examples of certain molecular vibrational modes, in Benzene for example,[32] which fluctuate as slowly as 10THz. If activated states of these vibrational modes are important to the rate of a particular reaction, the details of a substrate's phonon spectrum, not present in a Markovian Langevin simulation, may become relevant.

Methods

Langevin simulations

The 2D Langevin simulations were performed with a $\Delta t =$ 1fs time step for a total of up to 2µs of simulation run time spread over $100 - 200$ separate 10ns trajectories. At each time step, the background force on the adatom was determined through the gradient of the background potential, as interpolated using a bi-cubic spline on the 100×100 grid provided in the Supplemental Information. The random force was sampled independently for each force component from a zero-mean Gaussian random variable with standard deviation $\sigma/\sqrt{\Delta t}$ where the relevant fluctuation dissipation relation sets σ through $\langle f(t_1) f(t_2)\rangle = \sigma^2 K(|t_1 - t_2|)$. In the non-Markovian simulations, convolution with a discretized exponential memory kernel was performed through the relation

$$\int_0^{t_n} dt' K(t-t')\,\dot{\vec{r}}(t') \approx \alpha \int_0^{t_{n-1}} dt' K(t-t')\,\dot{\vec{r}}(t') + \frac{1}{1-\alpha}\dot{\vec{r}}(t_n) \tag{12}$$

where $\alpha = \exp\frac{-\Delta t}{\tau}$. A colored noise spectrum was produced by generating an uncorrelated sequence of impulses and performing an equivalent discretized convolution with $K(t)$, this trick is only valid for an exponential memory kernel. At each time-step, the net force was determined as the sum of the background force, noise force, and the relevant friction law and the adatom position and velocity were propagated forwards in time using a Velocity-Verlet integrator.[33]

3D molecular dynamics simulations

The 3D molecular dynamics simulation was constructed in a similar fashion to the simulation constructed by Ellis[30] and used the same substrate force constant and Morse potential parameters. The key difference is that a larger

$8 \times 8 \times 8$ substrate was used and the pairwise adatom interactions with the substrate atoms were tracked up to a separation of 3.1 times the Morse potential parameter r_0 in separation. A Velocity Verlet integrator[33] with a 10fs time step was used to propagate the simulation through time for 200 runs of 10ns at 300K.

Extracting the 2D background potential

The 3D simulation was used to produce 2µs of adatom trajectory at 8 temperatures across the range $140-300$K. The 2µs trajectory of each temperature was mapped back into the first 2D unit cell on the periodic surface and binned into a 100×100 2D grid, ignoring the co-ordinate perpendicular to the substrate. Using Eq. 5, the 2D free energy was calculated and verified not to vary as a function of temperature. The potential grid provided in the supplemental information and shown in Fig. 1 is the arithmetic mean of these grids.

Code availability

All code was written in a combination of Python and Cython and is available on GitHub through the link `https://github.com/jjhw3/gle_research`. If this manuscript is accepted for publication I will provide a condensed version of the code as this repository was used for many sub-projects relating to Langevin and Molecular Dynamics simulations and therefore contains some clutter.

Data availability

The trajectories of all 3D molecular dynamics simulations are available upon request. The trajectories of the Langevin simulations were not stored due to storage space constraints, however, equivalent trajectories may be quickly recomputed using $\sim$ 15000 CPU hours on current computing cluster hardware. The ensemble average of the total energy autocorrelation function and the ISF at $\Delta K = 1.23\text{Å}^{-1}$ is available for each Langevin simulation upon request. The potential energy surface, U_{free}, is available in the supplemental information.

References

[1] Andrew P. Jardine, Shechar Dworski, Peter Fouquet, Gil Alexandrowicz, David J. Riley, Gabriel Y. H. Lee, John Ellis, and William Allison. Ultrahigh-resolution spin-echo measurement of surface potential energy landscapes. *Science*, 304(5678):1790–1793, June 2004.

[2] A Jardine, G Alexandrowicz, H Hedgeland, W Allison, and J Ellis. Studying the microscopic nature of diffusion with helium-3 spin-echo. *Physical chemistry chemical physics : PCCP*, 11:3355–74, 06 2009.

[3] A.P. Jardine, H. Hedgeland, G. Alexandrowicz, W. Allison, and J. Ellis. Helium-3 spin-echo: Principles and application to dynamics at surfaces. *Progress in Surface Science*, 84:323–379, 11 2009.

[4] Barbara A. J. Lechner, Holly Hedgeland, Andrew P. Jardine, William Allison, B. J. Hinch, and John Ellis. Vibrational lifetimes and friction in adsorbate motion determined from quasi-elastic scattering. *Physical Chemistry Chemical Physics*, 17(34):21819–21823, 2015.

[5] G. Alexandrowicz, A. P. Jardine, P. Fouquet, S. Dworski, W. Allison, and J. Ellis. Observation of microscopic co dynamics on cu(001) using ^{3}He spin-echo spectroscopy. *Phys. Rev. Lett.*, 93:156103, Oct 2004.

[6] H. Hedgeland, P. Fouquet, A. P. Jardine, G. Alexandrowicz, W. Allison, and J. Ellis. Measurement of single-molecule frictional dissipation in a prototypical nanoscale system. 5(8):561–564, July 2009.

[7] Anton Tamtögl, Emanuel Bahn, Jianding Zhu, Peter Fouquet, John Ellis, and William Allison. Graphene on ni(111): Electronic corrugation and dynamics from helium atom scattering. *The Journal of Physical Chemistry C*, 119(46):25983–25990, November 2015.

[8] Peter Stephen Morris Townsend. *Diffusion of light adsorbates on transition metal surfaces*. PhD thesis, 2018.

[9] Marco Sacchi, Pratap Singh, David Chisnall, David Ward, Andrew Jardine, Bill Allison, John Ellis, and Holly Hedgeland. The dynamics of benzene on cu(111): a combined helium spin echo and dispersion-corrected dft study into the diffusion of physisorbed aromatics on metal surfaces. *Faraday Discuss.*, 204, 08 2017.

[10] Anton Tamtögl, Marco Sacchi, Nadav Avidor, Irene Calvo-Almazán, Peter S. M. Townsend, Martin Bremholm, Philip Hofmann, John Ellis, and William Allison. Nanoscopic diffusion of water on a topological insulator. *Nature Communications*, 11(1), January 2020.

[11] H.A. Kramers. Brownian motion in a field of force and the diffusion model of chemical reactions. *Physica*, 7(4):284–304, 1940.

[12] R. Zwanzig. *Nonequilibrium Statistical Mechanics*. Oxford University Press, 2001.

[13] R Kubo. The fluctuation-dissipation theorem. *Reports on Progress in Physics*, 29(1):255–284, 1966.

[14] Simon P. Rittmeyer, David J. Ward, Patrick Gütlein, John Ellis, William Allison, and Karsten Reuter. Energy dissipation during diffusion at metal surfaces: Disentangling the role of phonons versus electron-hole pairs. *Physical Review Letters*, 117(19), November 2016.

[15] S. K. Sinha. Lattice dynamics of copper. *Phys. Rev.*, 143:422–433, Mar 1966.

[16] R. Ramji Rao and C. S. Menon. Lattice dynamics, third-order elastic constants, and thermal expansion of titanium. *Phys. Rev. B*, 7:644–650, Jan 1973.

[17] J. Zarestky and C. Stassis. Lattice dynamics of γ-fe. *Phys. Rev. B*, 35:4500–4502, Mar 1987.

[18] R. Stedman and G. Nilsson. Dispersion relations for phonons in aluminum at 80 and 300°k. *Physical Review*, 145(2):492–500, May 1966.

[19] J. Ellis, J. P. Toennies, and G. Witte. Helium atom scattering study of the frustrated translation mode of co adsorbed on the cu(001) surface. *The Journal of Chemical Physics*, 102(12):5059–5070, 1995.

[20] Patrick Senet, Jan Peter Toennies, and Gregor Witte. Low-frequency vibrations of alkali atoms on cu(001). *Chemical Physics Letters*, 299:389–394, 1999.

[21] Frank Hofmann and J. Peter Toennies. High-resolution helium atom time-of-flight spectroscopy of low-frequency vibrations of adsorbates. *Chemical Reviews*, 96(4):1307–1326, 1996. PMID: 11848791.

[22] B. N. Brockhouse, T. Arase, G. Caglioti, K. R. Rao, and A. D. B. Woods. Crystal dynamics of lead. i. dispersion curves at 100°k. *Phys. Rev.*, 128:1099–1111, Nov 1962.

[23] J. R. D. Copley and B. N. Brockhouse. Crystal dynamics of rubidium. i. measurements and harmonic analysis. *Canadian Journal of Physics*, 51(6):657–675, March 1973.

[24] Peter S M Townsend and David J Ward. The intermediate scattering function for quasi-elastic scattering in the presence of memory friction. *Journal of Physics Communications*, 2(7):075011, jul 2018.

[25] Nathan E Glatt-Holtz, David P Herzog, Scott A McKinley, and Hung D Nguyen. The generalized langevin equation with power-law memory in a nonlinear potential well. *Nonlinearity*, 33(6):2820–2852, April 2020.

[26] T. G. Mason and D. A. Weitz. Optical measurements of frequency-dependent linear viscoelastic moduli of complex fluids. *Phys. Rev. Lett.*, 74:1250–1253, Feb 1995.

[27] Eliza M. McIntosh, K. Thor Wikfeldt, John Ellis, Angelos Michaelides, and William Allison. Quantum effects in the diffusion of hydrogen on ru(0001). *The Journal of Physical Chemistry Letters*, 4(9):1565–1569, April 2013.

[28] M Diamant, S Rahav, R Ferrando, and G Alexandrowicz. Interpretation of surface diffusion data with langevin simulations: a quantitative assessment. 27(12):125008, mar 2015.

[29] G. Alexandrowicz, A. P. Jardine, H. Hedgeland, W. Allison, and J. Ellis. Onset of 3d collective surface diffusion in the presence of lateral interactions: Na/Cu(001). *Phys. Rev. Lett.*, 97:156103, Oct 2006.

[30] J. Ellis and J.P. Toennies. A molecular dynamics simulation of the diffusion of sodium on a cu(001) surface. *Surface Science*, 317(1):99–108, 1994.

[31] C T Chudley and R J Elliott. Neutron scattering from a liquid on a jump diffusion model. 77(2):353–361, feb 1961.

[32] Shaoqing Wang. Intrinsic molecular vibration and rigorous vibrational assignment of benzene by first-principles molecular dynamics. *Scientific Reports*, 10(1), October 2020.

[33] Loup Verlet. Computer "experiments" on classical fluids. i. thermodynamical properties of lennard-jones molecules. *Phys. Rev.*, 159:98–103, Jul 1967.